Thin Hf layers in Nb studied by the perturbed angular correlation method.
I. Characterization of thin layers in Nb-Hf-Nb layered structures

P. Ziegler and Y. Q. Sheng*

Fakultät für Physik, Universität Konstanz, Universitätsstrasse 1, Postfach 55 60,
D-7750 Konstanz 1, Federal Republic of Germany

O. Boebel, J. Steiger, and A. Weidinger

Hahn-Meitner-Institut Berlin G.m.b.H., Glienickerstrasse 100,
D-1000 Berlin 39, Federal Republic of Germany

Nb-Hf-Nb sandwich samples were prepared by electron-gun evaporation. The thickness of the Hf layers ranged from 1 to 200 nm. The structural properties were studied with use of the perturbed angular correlation method. The measurements show that the Hf layers with thicknesses larger than 20 nm are oriented with the c axis of the hcp structure parallel to the surface normal. If the thickness of the Hf layer is smaller than 20 nm, the layer is strongly disturbed.

I. INTRODUCTION

Metallic multilayers have been produced over the past few years by sputtering and electron-beam evaporation. The structure of multilayers such as Cu-Ni,[1] Nb-Cu,[2,3] Nb-Ta,[4,5] Nb-Ti,[6] and Nb-Zr (Refs. 7 and 8) was worked out mostly by x-ray scattering. According to Claeson et al.,[8] the Zr layers show a gradual hcp to bcc transformation as the layer spacing decreases in the Nb-Zr multilayer system, being predominantly hcp for $\Lambda \gg 5$ nm and predominantly bcc for $\Lambda \ll 5$ nm. In addition, the layers are not sharp since there is a significant interdiffusion. It can be expected that the system Nb-Hf shows a similar behavior since Hf and Zr have almost identical material properties.

In the present experiment, Nb-Hf-Nb sandwich samples were made by electron-gun evaporation and the study was performed by the perturbed angular correlation (PAC) method. In this paper, we report the results obtained on the structure of the evaporated Hf layer in the Nb-Hf-Nb sandwich; in paper II, the effects that are imposed on the system by hydrogen charging will be presented.

II. PREPARATION OF THE SAMPLES

The investigated samples were sandwiches of Nb-Hf-Nb with different thicknesses of the Hf layers. The Hf layer (source purity 97%, impurity mainly Zr) was evaporated with an electron gun in ultrahigh vacuum ($p < 10^{-7}$ Pa) on a Nb-foil substrate.

Preceding the evaporation of Hf, the thin (20-μm) high-purity Nb-foil substrate (Ta impurities less than 10 wt. ppm) from the Max-Planck-Institut für Metallforschung Stuttgart was annealed ($T \simeq 2300$ K) in ultrahigh vacuum in order to remove the oxide layer from the surface and a 10–50-nm-thick Nb layer was evaporated onto the substrate. The substrate temperature was 300 K during the evaporation of both Nb and Hf. X-ray diffraction showed that the Nb foil had a (110) surface.

The thickness of the Hf layer was monitored with a quartz oscillator and had values between 1 and 200 nm. The evaporation rate of Hf was 0.1–0.5 nm/s and that of Nb 0.1–1.0 nm/s. Finally, the sample was sealed by evaporating a 500-nm-thick Nb layer. After the sealing, the sample was removed from the vacuum chamber and sent to a reactor for neutron activation. By the nuclear reac-
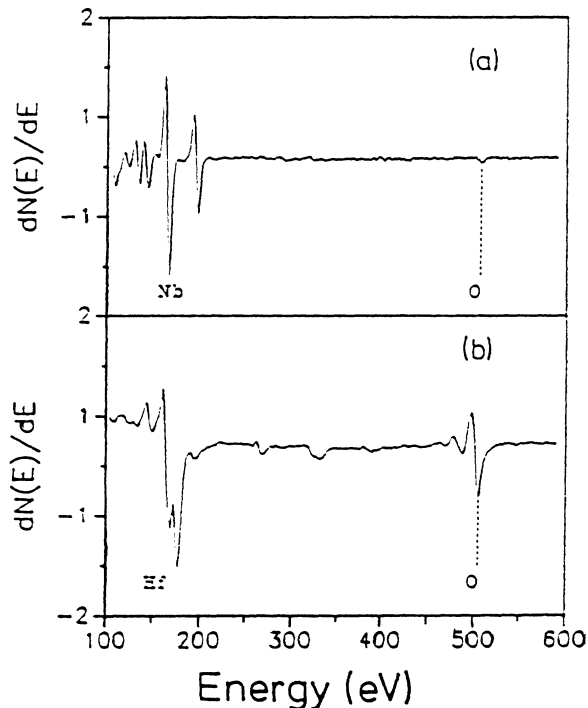

FIG. 1. AES spectra of evaporated Nb (a) and Hf (b) layers. The layer thicknesses were 10 and 50 nm, respectively. The oxygen signals correspond in both cases to a contamination of approximately 5%.
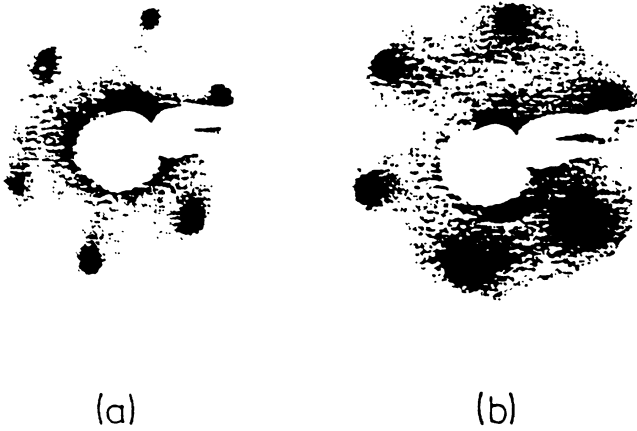
FIG. 2. LEED patterns of evaporated Nb (a) and Hf (b) layers. The layer thicknesses were 10 and 50 nm, respectively. The bcc (110) surface structure of Nb and the hexagonal closed-packed structure of Hf can be seen.

FIG. 3. Four-detector PAC setup and the orientation of the surface normal $\vec{n}$ of the sandwich sample with respect to the detector system defined by the angles ϑ and φ.

tion ^{180}Hf(n,γ) ^{181}Hf radioactive probe atoms are generated in the Hf layer. The subsequent PAC measurement is sensitive only to these probe atoms.

The purity and structure of the films was checked by Auger-electron spectroscopy (AES) and low-energy electron diffraction (LEED). The data shown in Figs. 1 and 2 were taken after the evaporation of a 10-nm Nb layer onto the Nb substrate and after the subsequent evaporation of a 50-nm Hf layer, respectively. The major contaminant (see Fig. 1) is oxygen, which amounts to about 5% for Nb and Hf. The LEED spectrum of the Nb layer shows that monocrystalline regions with a (110) orientation of the surface are formed [Fig. 2(a)]. For the evaporated Hf layer, LEED reflexes were observed only for films thicker than 5 nm. As an example, the LEED pattern of a 50-nm-thick Hf layer is shown in Fig. 2(b). The hexagonal closed-packed structure is clearly seen.

III. PAC METHOD

In our experiment, the perturbed angular correlation (PAC) technique with the radioactive-probe nucleus ^{181}Hf that decays to ^{181}Ta was used.[9,10] The PAC system was a conventional four-detector setup with fast-slow coincidences. The spectra for the different start-stop detectors (Fig. 3) were combined by forming ratios of the form

$$R(t)=\frac{2}{3}\left[\left[\frac{N_{13}(180°,t)N_{31}(180°,t)}{\alpha N_{14}(90°,t)N_{32}(90°,t)}\right]^{1/2}-1\right], \quad (1)$$

with equivalent 180° and 90° spectra, respectively. Here $N_{ij}(\theta,t)$ are the coincidence count rates between detector i and j corrected for accidental coincidences. θ is the angle between the emission directions of γ rays registered in detector i and j and t is the time elapsed between the arrival of γ_1 and γ_2 of the $\gamma\gamma$ cascade. α in (1) is a normalization constant that accounts for the different efficiencies and solid angles of the detectors involved and was determined by requiring that $R(t=0)$ of (1) is equal to $R(t=0)$ of the standard expression where the combina-
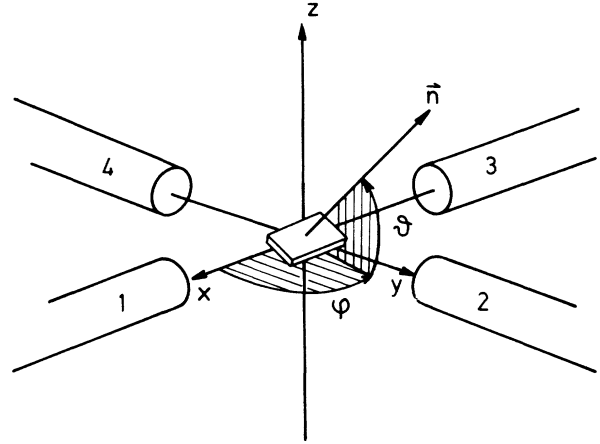
tions $(i,j)=(1,3)$, (2,4), (1,4), and (2,3) are used in (1). This later expression is independent of the detector efficiencies and solid angles (i.e., $\alpha=1$) and therefore can be used to determine α in (1) since at $t=0$ both expressions must give the same value. The actual value of $R(t=0)$ was determined by an extrapolation of $R(t)$ from $t>0$ to $t=0$.

The experimental $R(t)$ spectra formed according to expression (1) or other possible detector combinations were fitted with the theoretical function

$$R(t)=A_{\text{eff}}G_{\text{eff}}(t), \quad (2)$$

where A_{eff} is an effective anisotropy of the $\gamma\gamma$ correlation and $G_{\text{eff}}(t)$ has the form (for spin $I=\frac{5}{2}$)

$$G_{\text{eff}}(t)=s_0+\sum_{n=1}^{3}s_n e^{-\delta\omega_n t}\cos(\omega_n t). \quad (3)$$

The ω_n in (3) correspond to the transition energies in the intermediate state; they are uniquely related to the electric-field gradient (EFG) causing the splitting of the state. The exponential factor in (3) accounts for a possible distribution of the EFG; here a Lorentzian distribution with relative width δ was assumed. The coefficients s_0 and s_n can be calculated if the relative orientations of the detectors and the EFG axes are known. On the other hand, for an a priori unknown orientation, a comparison of the experimentally determined values with the calculated ones can be used to determine the EFG axes.

In the analysis of (1) with expressions (2) and (3) the following parameters were fitted: A_{eff}, s_0, s_n, δ and ω_n with the restrictions $s_0+s_1+s_2+s_3=1$ and $\omega_3=\omega_1+\omega_2$. From the ω_n's the quadrupole interaction constant

$$\nu_Q=\frac{eQV_{zz}}{h} \quad (4)$$

and the asymmetry parameter

$$\eta=(V_{xx}-V_{yy})/V_{zz} \quad (5)$$

were calculated by a well-known procedure.[9] Here, Q is

the quadrupole momentum of the intermediate state ($Q = 2.53$ b for the $\frac{5}{2}^+$ state of ^{181}Ta) and V_{ii} are the components of the EFG tensor in the principle axes frame. Finally, the spread of the interaction strength Δv_Q was calculated by setting

$$\delta = \Delta v_Q / v_Q . \tag{6}$$

IV. EXPERIMENTAL RESULTS AND DISCUSSION

A. Oriented growth of Hf films on Nb foils

In PAC experiments[9,10] the correlation between the 133- and 482-keV γ rays of ^{181}Ta after the β decay of ^{181}Hf is measured as a function of time. Without an electric-field gradient at the probe site, this correlation is time-independent and shows a constant anisotropy of approximately -0.18 for our arrangement. In order to determine whether the Hf layer has an oriented growth, a series of measurements were performed with varying sample-detector arrangements (see Fig. 3).

In Fig. 4 some typical PAC spectra together with their Fourier transforms of a Nb-Hf-Nb sample ($d_{\mathrm{Hf}} = 70$ nm) are shown for three different orientations of the Hf layer normal $\vec{n}$ with respect to the detector plane at room temperature. Since the isomeric nuclear state in ^{181}Ta, populated by the β decay of ^{181}Hf, has the spin $I = \frac{5}{2}$, three transition frequencies occur for each electric-field gradient. The relative intensities of these three frequencies are clearly orientation dependent and therefore indicate that the film has a preferred axis.

In Fig. 5 the frequency amplitudes s_n extracted from the data by fitting the time spectra are plotted for the

FIG. 5. Comparison of the calculated amplitudes s_n of the transition frequencies ω_n with the experimental data for a Nb-Hf-Nb sandwich sample ($d_{\mathrm{Hf}} = 70$ nm) under the assumption that the c axis of the Hf layer is parallel to the normal. In the figure, only the case for $\vartheta = 0°$ and different φ is demonstrated for clarity.

different angles. The solid curves presented in Fig. 5 have been calculated for an electrical-field gradient pointing along the surface normal taking into account the finite solid angles for the γ detectors. The calculations were done for $\eta = 0.35$ (experimental value) and averaged over the x-y orientations.

The good agreement of the theoretical curves with the experimental data establishes that the c axis of the electric-field gradient of the Hf layer is directed parallel to the surface normal indicating an oriented growth of the Hf layer. This is in agreement with the LEED pattern seen in Fig. 2(b).

The interaction parameters extracted from the PAC spectra and averaged over all measurements are $v_Q = 300 \pm 15$ MHz and $\eta = 0.35 \pm 0.05$. These quantities are in good agreement with those known from the bulk
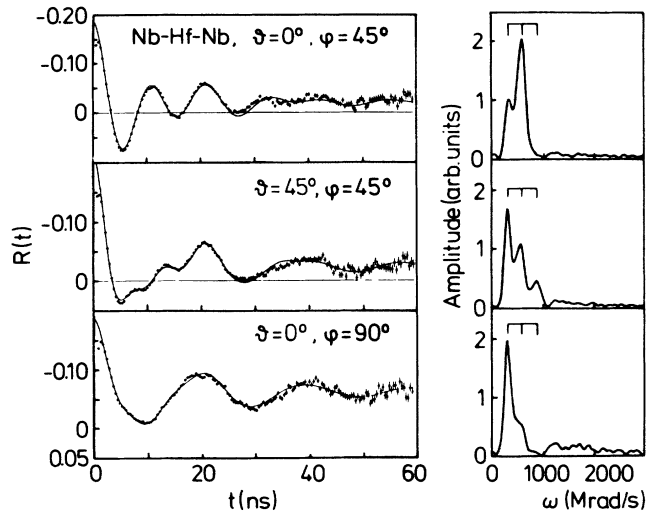

FIG. 4. Typical PAC spectra and their Fourier transforms for a 70-nm-thick Hf layer in a Nb-Hf-Nb sandwich sample. For clarity reasons, the $\omega = 0$ contribution in the Fourier spectra was suppressed by subtracting a constant value in the $R(t)$ spectra before the transformation. The spectra show a strong dependence on the angle between the detector axis and the normal of the foil. The analysis of the angular dependence shows that the c axis is parallel to the normal of the foil (see text).
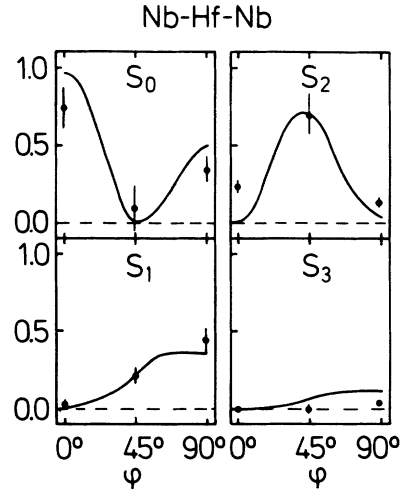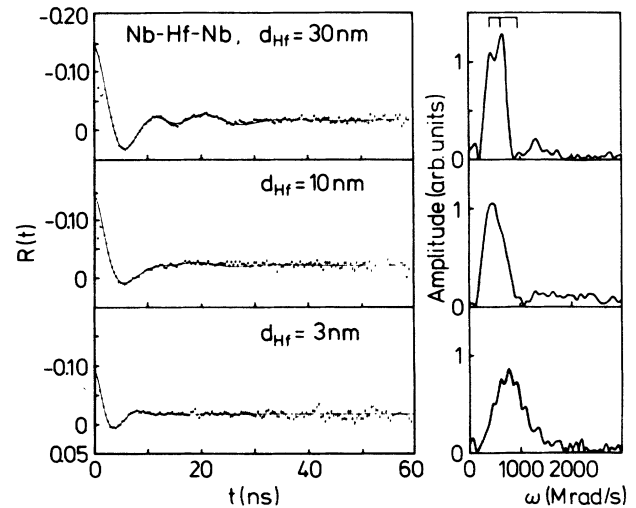

FIG. 6. Three typical PAC spectra and their Fourier transforms for three Nb-Hf-Nb samples with different thicknesses of the Hf layers.
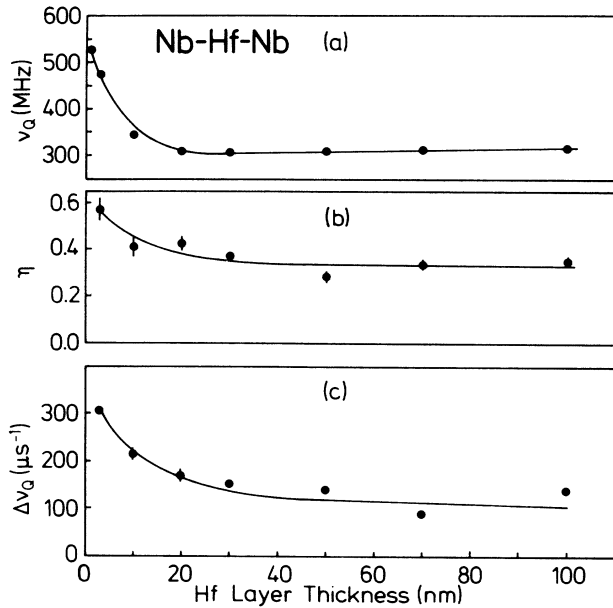
FIG. 7. Dependence of the interaction parameters on the Hf layer thickness. (a) quadrupole interaction constant v_Q; (b) asymmetry parameter η; (c) width (Δv_Q) of the distribution of the interaction constants.

Hf samples.[11] Thus the evaporated Hf film, here with a thickness of 70 nm, has—within the experimental errors—the bulk properties of single-crystalline Hf. The deviation of η from $\eta=0$, the value expected for a pure Hf hcp structure is usually[11] attributed to the rather high-Zr content (3 at. %) that disturbs the local axial symmetry at the probe site.

B. Dependence of the electrical-field gradient on the Hf layer thickness

PAC spectra with parameters as in bulk Hf are obtained for films with thicknesses above 20 nm. An example is shown in the upper spectrum of Fig. 6 for a Hf film with a thickness of 30 nm. For thinner films, strong deviations from this behavior were found. The spectrum in the middle of Fig. 6 for a film with $d_{Hf}=10$ nm shows that the structure in the PAC spectrum becomes smeared

out but the centroid of the frequency distribution remains the same as in the thicker films. For even thinner layers $(d_{Hf}=3$ nm, lower spectrum in Fig. 6) the centroid shifts to higher frequencies.

The parameters extracted from the data are displayed in Fig. 7. It can be seen that the deviation from the bulk behavior sets in at around 20-nm layer thickness. We find that the strength of the interaction (v_Q) as well as the width (Δv_Q) increase drastically below $d_{Hf}=20$ nm. This indicates that these films are highly disturbed and that the local structure deviates strongly from the bulk behavior of Hf. Possible reasons for these disturbances are local defects, impurities, or intermixing of Hf and Nb at the interface. The PAC method cannot distinguish between these possibilities.

V. CONCLUSION

The PAC method is well suited to study structural properties of evaporated thin films. We find that Hf layers on Nb foils grow oriented with the c axis parallel to the surface normal. The Hf layer shows bulk properties if its thickness exceeds 20 nm. Thinner films are strongly distorted. The reason of the disturbance can be associated with a disordered arrangement of atoms and/or intermixing of Nb and Hf in the surrounding of the interface, with a significant concentration of defects and/or impurities in the layer.

*Permanent address: Department of Applied Physics, Shanghai Jiao Tong University, 1954 Hua Shan Road, Shanghai 200030, People's Republic of China.

[1]E. M. Gyorgy, D. B. McWhan, J. F. Dillon, L. R. Walker, and J. V. Wasczak, Phys. Rev. B 25, 6739 (1982).

[2]W. P. Lowe, T. W. Barbee, T. H. Geballe, and D. B. McWhan, Phys. Rev. B 24, 6193 (1981).

[3]I. K. Schuller, Phys. Rev. Lett. 44, 1597 (1980).

[4]S. M. Durbin, J. E. Cunningham, M. E. Mochel, and C. P. Flynn, J. Phys. F 11, L223 (1981).

[5]G. Hertel, D. B. McWhan, and J. M. Rowell, in Superconductivity in d- and f-band metals 1982, edited by W. Buckel and W. Weber (Kernforschungszentrum Karlsruhe GmbH.,

Karlsruhe, West Germany, 1982).

[6]J. Q. Zheng, J. B. Ketterson, C. M. Falco, and I. R. Schuller, Physica B+C (Amsterdam) 108B, 945 (1981).

[7]W. P. Lowe and T. H. Geballe, Phys. Rev. B 29, 4961 (1984).

[8]I. Claeson, J. B. Boyce, W. P. Lowe, and T. H. Geballe, Phys. Rev. B 29, 4969 (1984).

[9]H. Frauenfelder and R. M. Steffen in Alpha-, Beta-, and Gamma-ray Spectroscopy, edited by K. Siegbahn (North-Holland, Amsterdam, 1966), Vol. 2.

[10]A. Weidinger, J. Less-Common Met. 103, 285 (1984).

[11]R. L. Rasera, T. Butz, A. Vasquez, H. Ernst, G. K. Shenoy, B. D. Dunlap, R. C. Reno, and G. Schmidt, J. Phys. F 8, 1579 (1978).